
ARTICLE

Reactivity-Initiated-Accident Analysis without Scram of a Molten Salt Reactor

Nobuhide SUZUKI^{1,*} and Yoichiro SHIMAZU²

¹Mitsubishi Heavy Industries, Ltd, 1-1, Wadasaki-cho 1-chome, Hyogo-ku, Kobe 652-8585, Japan

²Graduate School of Engineering, Hokkaido University, Kita 13, Nishi 8, Kita-ku, Sapporo 060-8628, Japan

(Received August 29, 2007 and accepted in revised form February 18, 2008)

Recently, a conceptual design of a small MSR, named FUJI-12 has been proposed. FUJI-12 operates with the same fuel salt as the Molten Salt Breeder Reactor (MSBR) designed by ORNL. The authors are interested in the MSR concept due to its high potential in the areas of safety, proliferation resistance, resource sustainability and waste reduction, all necessary requirements for the generation IV nuclear power systems. The authors believe that additional investigations are necessary for future study. From this point of view, the authors have analyzed various reactivity insertion accidents due to control rod malfunctions in FUJI-12. The MSR can be operated with a small excess reactivity. However, at the same time, the delayed neutron fraction is quite small due to the usage of U-233 as fissile material and the circulation of the fuel salt. Therefore, the reactivity insertion accident should be qualitatively evaluated. The reactor transients were analyzed without scram in order to evaluate the severity of such accidents against the safety. Although the total primary system design of FUJI-12 is not completed, and thus, the accident analyses include some crude assumptions, it can be expected that the reactivity insertion accident in FUJI-12 would not result in severe plant conditions.

KEYWORDS: molten salt reactor, reactivity-initiated accident, transient without scram, reactor safety, control rod malfunction, reactivity coefficient, safety analysis

I. Introduction

Molten Salt Reactors (MSRs) have a long history with the first design studies beginning in the 1950s at the Oak Ridge National Laboratory (ORNL). One of the results from these early and extensive studies was reported in ORNL-4541,¹⁾ entitled “Conceptual Design of a Single Fluid Molten Salt Breeder Reactor.” However, the developmental efforts have slowed considerably except in Russia, France, Japan^{2,3)} and a few other places carrying out small-scale development. Recently, a conceptual design of a small MSR, named FUJI-12^{4,5)} has been proposed. FUJI-12 operates with the same fuel salt as the Molten Salt Breeder Reactor (MSBR) designed by ORNL. The fuel salt is ⁷LiF-BeF₂-ThF₄-UF₄ (71.7-16-12-0.3 mole%). However, it differs from the ORNL design in several ways, such as no on-site chemical processing plant and a low rated power. The authors are interested in the MSR concept due to its high potential in the areas of safety, proliferation resistance, resource sustainability and waste reduction, all necessary requirements for the generation IV nuclear power systems as stated in “A Technology Roadmap for Generation IV Nuclear Energy Systems,” GIF-002-00, Dec.(2002) by U.S. DOE. Therefore

the MSR concept has been selected as one of the promising candidates for future consideration.

As described above, the fuel salt is circulated in the reactor loop. This results in decreasing the delayed neutron fraction due to the loss of delayed neutrons flown out of the reactor. Furthermore, the delayed neutron fraction of uranium-233 is quite smaller than that of the other fissile materials. In the present study, the fissile material was conservatively assumed as uranium-233 for simplicity. Thus, the addition of positive reactivity might result in serious transient. From this point of view, accidents of positive reactivity addition were analyzed using a reactor simulator based on a detailed r-z two-dimensional neutron diffusion model coupled with thermal/hydraulic calculations. The analysis is still preliminary and the assumptions are relatively crude because the developmental activities on MSRs have been sparse. Since there are few theoretical or experimental data available for detailed analyses, we used simple assumptions and data previously published.¹⁾ However, such a preliminary study can give us information about necessary and indispensable data for the detailed system design that can be applied in future accident analyses. Moreover, it might be helpful to know the worst case transient in order to plan countermeasures against such an accident. From the licensing point of view, it is permitted to assume reactor scram in the analysis of design bases accidents. However, as described above, the

*Corresponding author, E-mail: shimazu@eng.hokudai.ac.jp

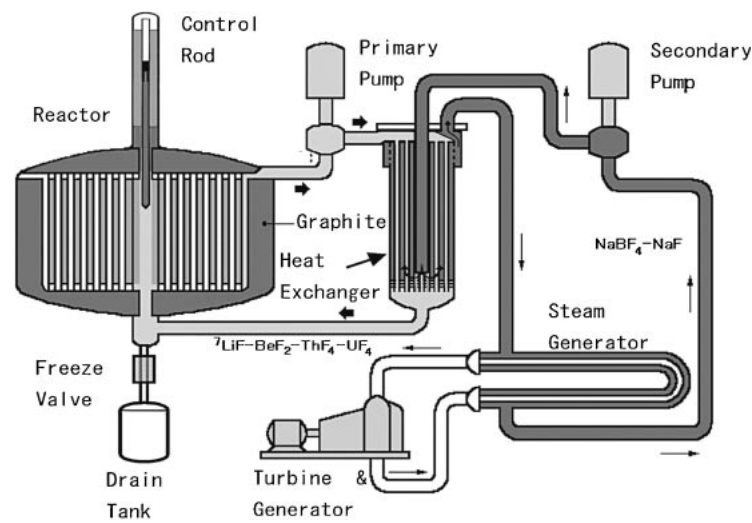


Fig. 1 Schematic view of FUJI-12

detailed plant system designs and scram conditions are not specified yet at present; we therefore assumed that no scram would take place. We do not claim that this accident represents the only possible accident in MSR. We will continue to investigate the safety of MSRs in the near future.

II. Description of FUJI-12 Design

A schematic design of the reactor core is shown in Fig. 1.⁶⁾ Note that an overflow line from the pump bowl to the drain tank is omitted in the figure. The overflow line is to be used when control rods are inserted and to replace the fuel salt in the core or to adopt fuel salt due to the expansion of the volume by temperature increase. The reactor is a graphite-moderated thermal reactor composed of the core and the reflector, consisting of many hexagonal prismatic elements made of high-density graphite. The size of the diagonal of the element is 20 cm and the radius of the center hole is 4.98 cm. The elements are surrounded by a neutron absorber made of boron carbide, and all these structures are contained in the reactor vessel made of modified Hastelloy-N. The fuel salt is made of LiF-BeF₂-ThF₄-UF₄. It flows into the reactor through the lower entrances at 840 K, flows upwards through passages in the graphite elements where the temperature increases due to nuclear fission reactions and then flows out of the reactor through the upper outlets at 980 K. The reactor can operate for an extended period without continuous fuel reprocessing and without graphite replacement in the core. The main design parameters are listed in Table 1. These parameters are typical values. The characteristics of MSRs are relatively independent of core lifetime. The specifications of the heat exchanger and the primary loop are also listed in Table 1. These parameters were evaluated by analogy with the design values of the MSBR.

III. Description of the Primary Loop Simulator

The authors developed a new simulator based on a reactor model in r-z geometry with an external loop of fuel salt cir-

Table 1 Principal design parameters of FUJI-12

Thermal Capacity	350 MWth
Net Electric Generation	150 MWe
Thermal Efficiency	43%
Number of Coolant Loops	2
Core	
Radius/Height	2.0/4.0 m
Graphite Fraction	70 vol%
Reflector	
Thickness Rad./Axi.	0.5/0.6 m
Graphite Fraction	99 vol%
Average Power Density	7.0 kWth/liter
Specifications of heat exchanger	
Thermal capacity	350 MW
Tube length	6.8 m
Total heat transfer area	760 m ²
Fuel salt volume	1.19 m ³
Fuel salt speed in heat exchanger	3.14 m/s
Fuel salt temperatures (Inlet/Outlet)	980 K/840 K
Coolant volume	7.25 m ³
Coolant speed	1.22 m/s
Coolant temperature (Inlet/Outlet)	765 K/670 K
Total length of primary loop	7.2 m
Fuel salt speed in primary loop	1.2 m/s
Fuel Salt	
Composition	
LiF	Balance
BeF ₂	16.0 mol%
ThF ₄	12.0 mol%
UF ₄	0.22 mol%
Volume in Reactor	
Total Volume	15.7 m ³
Flow Rate	20.2 m ³
Temperature Inlet/Outlet	0.55 m ³ /s 840 K/980 K

ulation and a heat exchanger for the MSR transient analysis. As the MSR has a completely radial symmetry and the fuel characteristics in the core are almost homogeneous, the r-z geometry can be applied to a wide range of core con-

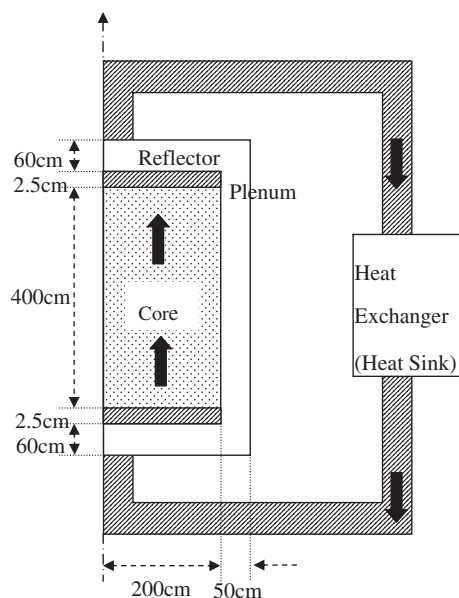


Fig. 2 Model for the calculation

figurations. The model for the calculation is shown in **Fig. 2**. The actual reactor geometry is such that the core radius is 200 cm and the height is 400 cm. The thicknesses of the radial and axial reflectors are 50 and 60 cm, respectively, and the width of the top and bottom plenums of the core is 2.5 cm each. The outer boundary of the reactor model is that of the axial and radial reflectors. It is based on a two-group neutron diffusion model with both reactor kinetics calculation and thermal analysis in the reactor. The numbers of calculation meshes of the reactor are 25 in the radial direction and 52 in the axial direction for reactor and reflector with a mesh size of 10 cm. The fuel plenum zones at the top and the bottom of the reactor are represented by a single mesh width of 2.5 cm.

The reactor kinetics is solved using the stiffness confinement method (SCM)⁷⁾ with a calculation time interval of 0.01 s together with the plant dynamics. Six-group delayed neutrons are considered and their precursors are calculated in each mesh based on the neutron flux in the mesh.

The reactivity feedback effect is taken into account in the temperature-dependent nuclear constants, which are calculated by the interpolation of tabulated nuclear constants. The procedure is the same as that installed in CITATION in SRAC95 developed by JAERI.⁸⁾ The temperature-dependent nuclear constants are calculated using the PIJ module of SRAC taking into account the fuel salt density change with temperature as described below. The temperature distributions of fuel salt and graphite blocks in the core are used to calculate the reactivity feedback for the neutronic calculation.

The temperature distributions are calculated by thermal and hydraulic analyses as follows. The circulation of the fuel salt in the reactor and the loops are also taken into account. The graphite core blocks have a central fuel passage with a diameter of about 10 cm. The fuel salt flows upward within this closed channel. Thus, the flow analysis uses a simple axial flow model. It assumes that some portion of the heat

Table 2 Delayed neutron constants

i (group)	β_i	λ_i (s $^{-1}$)
1	2.34171×10^{-4}	1.25964×10^{-2}
2	8.18020×10^{-4}	3.34000×10^{-2}
3	6.92913×10^{-4}	1.30706×10^{-1}
4	7.97878×10^{-4}	3.03222×10^{-1}
5	1.57349×10^{-4}	1.23167×10^{-0}
6	9.61766×10^{-5}	3.13831×10^{-0}

Table 3 Reactivity coefficients

Component	Reactivity coefficient
Fuel temperature	-0.00295 (% $\Delta k/k/K$)
Graphite temperature	$+0.00130$ (% $\Delta k/k/K$)
Void	0.091 (% $\Delta k/k/\%$ void)

from the fuel is transferred to the graphite moderator. The mesh sizes are the same as those for the neutron analysis.

The outer loop is divided into 140 equal-volume nodes. The heated molten fuel salt transfers the heat generated by fission to the primary heat exchanger and the cooled fuel salt is returned back to the reactor. The radial fuel flow distribution in the reactor is assumed to be such that the temperature rise in the reactor is homogeneous. The heat removal in the primary heat exchanger is assumed to be constant during the transient in order to obtain the severest results.

The nuclear constants were calculated using SRAC95. First of all, cell calculations for various graphite blocks with respective fuel passages were calculated using the SRAC-PIJ module. The nuclear data file was JENDL-3.2 and the number of energy groups was 107. Based on this calculation, two group nuclear constants were obtained for the core analyses. In MSRs, no burnup distribution exists and the core characteristics are not so time-dependent. The core-averaged kinetic parameters were obtained through the three-dimensional core calculation by CITATION and are listed in **Table 2**. Temperature and void reactivity coefficients are listed in **Table 3**.

IV. Reactivity-Initiated-Accident Analysis

1. Reactivity-Initiated Accident

The reactivity-initiated accident in the MSR is focused because the delayed neutron fraction is much smaller for the uranium-233 fissile material, and furthermore, some portion of delayed neutrons are lost from the core due to the circulation of fuel salt. Thus, even a small reactivity can be larger than that for prompt reactivity.

The MSR is equipped with four graphite control rods at the center of the reactor and inserted from the top of the reactor. The control rod insertion increases the thermalization of neutrons, and thus, results in positive reactivity addition. Given that the graphite density is about half of that of fuel

salt, the control rod insertion requires a certain driving force. The driving forces on the control rods in the MSR are the buoyancy from the fuel salt and the supporting force from the control system of the reactor. If the control system should lose the support of the control rods or the control rods should break, the control rods would be flown out of the reactor. Thus, in the MSR, accidental insertions can result from the malfunctions of the control rod drive mechanism and/or control rod control system or operator error.

The control rod maneuvering is expected for reactivity compensation during load changes. The fissile concentration adjustment is expected for reactivity loss due to core burnup. In the latter case, the requirement can be adjusted by varying the interval of the fuel salt composition control, and the speed of the reactivity addition could be limited. Thus, the reactivity-initiated accident of fast reactor transient could be expected to occur because of control rod insertion.

The speed of the control rod insertion could be varied depending on the extent of the malfunctions. In the previous study, based on a simple point reactor model, it has been shown that the severer transients are expected in the case of step reactivity addition than the ramp addition.⁹⁾ It is because the power pulse is larger in the step addition. Thus, in this paper, we assumed that the reactivity was added as a step for the severest case. Also, the scram was not expected during the transient and the heat sink was kept the same as that before the accident in order to obtain the severest results.

2. Reactivity Evaluation

The reactivities of one, two, three and four control rods worth were calculated based on the following assumptions. Each control rod is shaped in the form of an ordinal graphite moderator block with a center hole to cool the graphite. In other words, the diagonal of the element is 20 cm and the radius of the center hole is 4.98 cm. When one control rod is withdrawn, we assumed that the graphite volume was replaced by the same amount of fuel salt. The values of the control rod worth are listed in **Table 4**.

In MSRs, long-term reactivity adjustment will be accomplished by varying the fuel concentration. The reactivity effects to be controlled using the control rods are as follows. Reactivity swing from the rated power to zero power is 0.07%dk/k, which is based on the overall temperature coefficient of $-0.00165\%dk/k/K$ multiplied by the average temperature change of 40 K, which is half of the fuel salt temperature rise in the reactor.

The reactivity of equilibrium xenon is estimated based on the following consideration. Although the capability of the xenon stripping system has not been determined yet, it has been planned that a helium bubble injection system be instal-

led in FUJI-12 for stripping the gaseous fission products to reduce xenon poisoning.¹⁾ The poisoning effect of xenon is dependent on the system parameters such as bubble volume fraction in the fuel salt or the gas stripping efficiency. Taking into account the facts that the power density of FUJI-12 is one-third of that for MSBR and the fuel salt volume fraction in FUJI-12 is about twice of that for MSBR, the equilibrium xenon reactivity could be much smaller than 0.3%dk/k for MSBR. The effect of increase in bubble volume fraction was estimated in Ref. 12) such that when the volume fraction was increased from 0.2 to 0.4%, the poisoning decreased to 75%. Assuming that the capability of the system is the same as that of MSBR, the xenon reactivity will be about 0.075% dk/k ($= 0.3/3 \times 0.75$). However, in this study, it is assumed to be 0.1%dk/k.

Reactivity due to the change in the amount of gas entrained in the fuel salt is estimated as $\pm 0.02\%dk/k$, which is based on the assumption of sudden change in the gas volume by $\pm 100\%$ of the nominal value of 0.2% of the fuel salt with the void coefficient of 0.091%dk/k/%void.

Reactivity loss due to the circulation of fuel salt is calculated as follows. The point kinetic equations of six delayed neutron groups for circulating fuel reactor are expressed as follows.¹⁰⁾

$$\frac{dn(t)}{dt} = \frac{\rho_0 - \beta}{\ell} n(t) + \sum_{i=1}^6 \lambda_i C_i(t), \quad (1)$$

$$\begin{aligned} \frac{dC_i(t)}{dt} = & \frac{\beta_i}{\ell} n(t) - \lambda_i C_i(t) - \frac{1}{\tau_C} C_i(t) \\ & + \frac{\text{Exp}(-\lambda_i \tau_L)}{\tau_C} C_i(t - \tau_L), \end{aligned} \quad (2)$$

where

i : number of delayed neutron group, 1 to 6

$n(t)$: neutron flux

$C_i(t)$: concentration of i -th group delayed neutron precursor

β_i : fission yield of i -th group delayed neutron precursor

λ_i : decay constant of i -th group delayed neutron precursor

ℓ : neutron lifetime

ρ_0 : reactivity including bias for circulating fuel

τ_C : transit time of the fuel salt through core

τ_L : transit time of the fuel through external loop

The third term in the right-hand side of Eq. (2) indicates the rate of delayed neutron precursor flowing out of the core. The fourth term indicates also the delayed neutron precursor flowing in after the circulation of the external loop taking into account the decay during the circulation.

When the reactor is at its steady state, the left-hand sides of the equation are zero and the last parameter in Eq. (2) is equal to $C_i(t)$. We solve these equations for ρ_0 , which give the reactivity bias due to the fuel circulation. It is given as

$$\rho_0 = \sum_{i=1}^6 \beta_i \left[1 - \frac{\lambda_i}{\lambda_i + \frac{1}{\tau_C} (1 - \text{Exp}(-\tau_L \lambda_i))} \right]. \quad (3)$$

It means that with the circulation of fuel salt, criticality

Table 4 Control rods' reactivity

No. of control rods	ρ (% $\Delta k/k$)	ρ (in \$)
1	0.186	0.644
2	0.344	1.235
3	0.486	1.737

Table 5 Reactivity components

Component	Reactivity (%Δk/k)
Temperature	0.07
Xenon	0.10
Entrained gas	0.02
Fuel circulation	0.04

cannot be attained without this bias reactivity adjustment. The transit times of FUJI-12 in the core and the external loop are 28.5 and 8.1 s, respectively. These values can be calculated by dividing the salt volume in each region by the corresponding salt flow rate listed in Table 1. Based on this equation and using parameters for FUJI-12, it was found that the bias reactivity is 0.04%dk/k.

The reactivity effects discussed above are listed in Table 5. All the effects will not have maximum importance simultaneously and some will have an opposite sign. For example, when power is reduced, a negative reactivity is to be added. When power is reduced, then the xenon concentration will increase; thus, a positive reactivity must be added to compensate the reactivity loss. Thus, although the sum of all reactivity components becomes 0.23%dk/k, a total of 0.2%dk/k to be provided by the graphite control rods was expected to be adequate to cover the short-term reactivity effects.

The requirement for the reactivity control is expected to be approximately 0.2%dk/k. Then, based on the control rod worth calculation, this reactivity can be controlled using a control rod and a small portion of the second control rod. Therefore, we assumed that the maximum reactivity addition could occur with the malfunction of two control rods simultaneously.

3. Reactivity Addition at Zero Power Condition

The reactor was assumed to be critical with the power level of 0.001% of rated power without heat sink. The reactivity was assumed to be added by a step. After the initiation of the transient, we further assumed that the heat is not removed from the primary loop without scram. The relative power transients are shown in Fig. 3 for one and two control rod insertions, respectively. As can be seen, when two rods were inserted, a large power pulse of about four times of the rated power was generated. However, the fuel temperature was stabilized at approximately 1050 K at the maximum as shown in Fig. 4. Even when three control rods were inserted, the maximum temperature did not exceed 1200 K as shown in Fig. 4. The peak value of the power pulse reached about seventy.

When the fuel temperature rises, the volumes of both fuel salt and helium gas bubbles in the fuel salt circulated for fission gas stripping expand. Given that the thermal expansion of graphite is about two orders smaller than that of the fuel salt, it is neglected. The temperature dependence of the fuel salt is given as

$$D(g/cm^3) = 3.752 - 0.00068(T-273); \text{ T in Kelvin. (3)}$$

When the fuel salt temperature rises from 840 K to 1180 K,

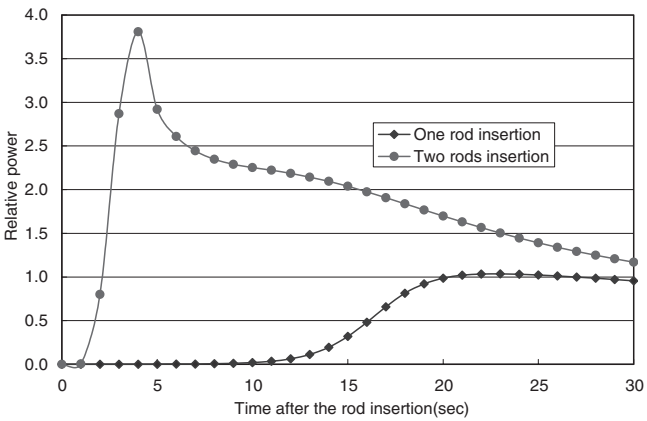


Fig. 3-1 Relative power transient at zero power condition up to 30 s

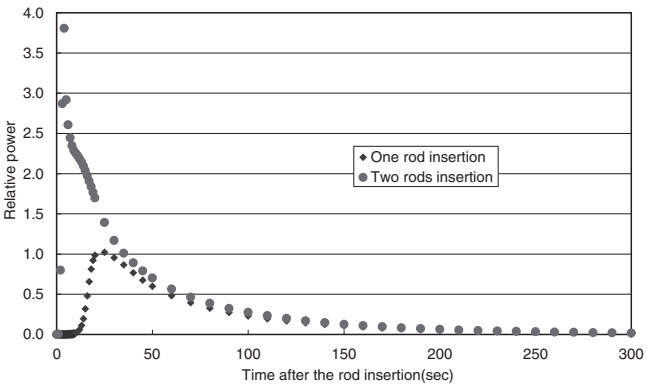


Fig. 3-2 Relative power transient at zero power condition

the density changes from 3.374 g/cm³ to 3.146 g/cm³, which means that the volume expands by about 7%. However, in the MSR loop, overflow lines are installed to absorb fuel expansion during normal operation or in emergency. Thus, the expansion of fuel can be mitigated. The volume of the helium bubbles at normal operation is estimated to be about 0.2% of the salt volume. For the same fuel temperature change, the helium volume expands by 43%. The void reactivity coefficient was estimated as 0.091 dk/k/%void. Thus, the positive reactivity addition is 0.0078%dk/k. This is negligibly small in comparison with the reactivity of the control rod. Thus, it is omitted in this study. These discussions are true for the next accident analysis.

4. Reactivity Addition at Full Power Condition

The reactor was assumed to be operating at the rated power at equilibrium condition. The reactivity was also added by a step. It was also assumed that the heat sink continued to be unchanged without reactor scram. The relative power transients for one and two control rod insertions are shown in Fig. 5. When two control rods were inserted, a power pulse of about 27 times of the rated power was generated in a very short time. This is because the accident was a reactivity accident. The temperature transients are shown in Fig. 6 for both cases. The maximum temperature exceeded 1200 K for about 250 s.

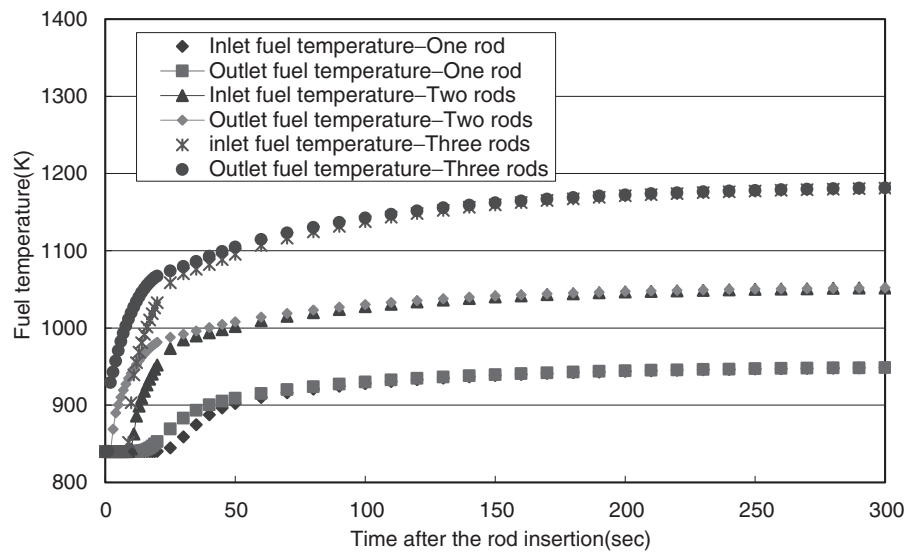


Fig. 4 Fuel temperatures during the transients at zero power

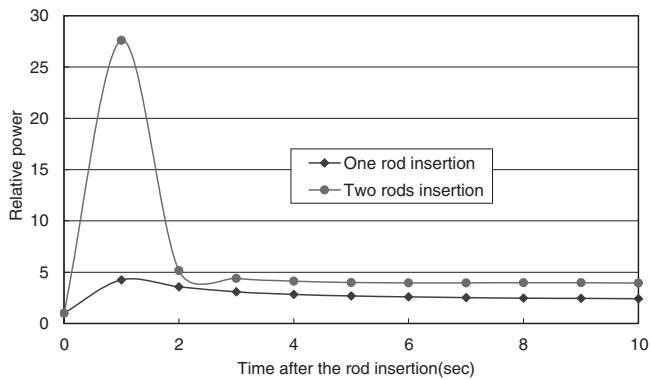


Fig. 5-1 Relative power transients at full power up to 10 s

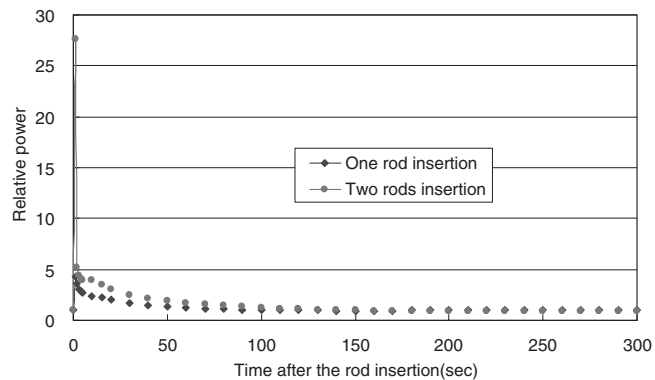


Fig. 5-2 Relative power transients at full power

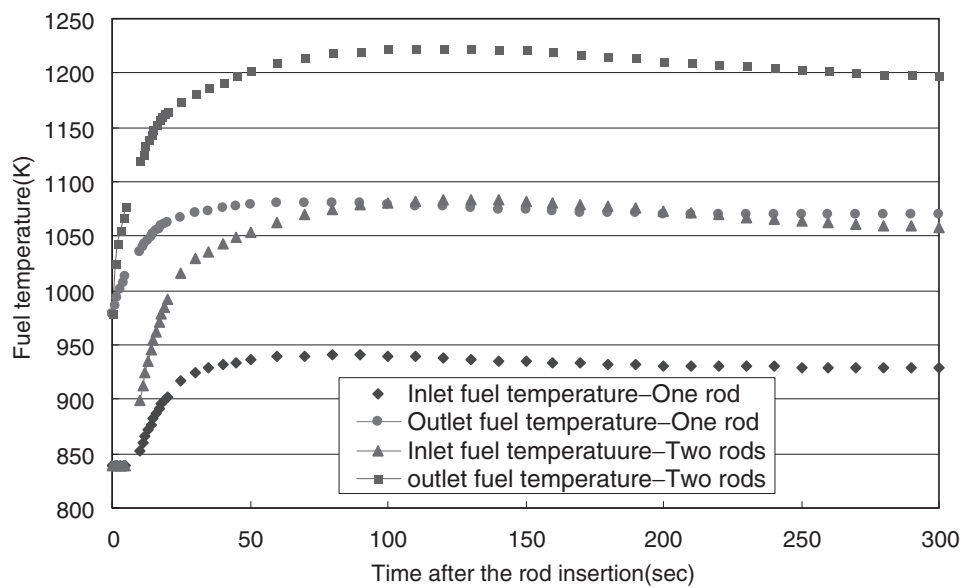


Fig. 6 Fuel temperature transients at full power

V. Discussion on the Safety Criteria for the MSBR

For MSRs, no explicit safety criteria have yet been established. In this study, we selected criteria based on the mechanical integrity of Hastelloy-N in order to avoid creep deformation based on the data of the Larson-Miller plot for Hastelloy-N.¹¹⁾ The stress intensity for the evaluation is assumed to be those for the MSBR.

A preliminary elastic stress analysis for the reactor vessel of the MSBR was performed by ORNL.¹⁾ Stress is due to the weights of salt, graphite and reactor vessel components and their thermal expansion. The analysis was based on the upper plenum of the vessel operating at 980 K and 0.39 MPa and the lower plenum at 866 K and 0.52 MPa. The maximum stress in the removable head due to pressure alone was 36.0 MPa. This stress was located in the reactor vessel head near the junction of the vessel head and shell. The maximum stress in the vessel occurred at the junction of the lower head and shell and was 123 MPa.

As the fuel salt temperature could rise into the creep range, the allowable temperature must be determined using both stress and the duration in which the stress is loaded. We conservatively chose the maximum duration to be 1 h, which is long enough to shut down the reactor and take corrective actions. The maximum stresses for both the top head and reactor vessel are assumed to be 43.2 and 148 MPa, respectively, with a calculation uncertainty of 20%. Finally, the allowable deformation during the interval of one hour is chosen to be 1%. Then, assuming that the temperature of Hastelloy-N is equal to that of the fuel salt, the allowable inlet and outlet temperatures are determined to be 1060 and 1200 K,¹⁰⁾ respectively.

VI. Conclusions

We have analyzed reactivity-initiated accidents at hot zero power and full power conditions without scram in the Molten Salt Reactor, FUJI-12. The maximum temperatures for inlet and outlet fuels were same at zero power condition. They were 950 and 1050 K, for one and two control rod withdrawals, respectively. When three control rods were withdrawn, the maximum temperature was 1180 K. The safety limiting temperature for the inlet fuel is 1050 K, and for the outlet fuel, 1200 K. Thus, it can be concluded that the safety limit is not violated for up to two control rod insertions at zero power.

The maximum fuel temperature for two rod insertions of 0.344%dk/k was 1220 K at the rated power. This result violates the safety limit. However, as discussed in the previous section, the maximum reactivity required for the normal

operation is expected to be less than 0.2%dk/k. Thus, the reactivity addition of two control rods of 0.344%dk/k is hardly expected. Therefore, it is concluded that the reactivity addition accident during normal operation will not result in safety violation. In other words, in order to ensure safety for reactivity-initiated accidents, the reactivity addition must be limited to less than that of two control rods worth. For example, the utilization of smaller sized control rods should be considered. If it could not be adopted, it could be said that some mitigation system might be installed to protect against the simultaneous control rod insertion. The other system to protect the reactor is an automated or passive salt drain system that has been designed for the MSBR.

References

- 1) R. C. Robertson, "Conceptual design study of a single-fluid molten-salt breeder reactor, ORNL-4541," Oak Ridge National Laboratory, Oak Ridge, TN (1971).
- 2) K. Furukawa, K. Minami, T. Oosawa, M. Ohta, N. Nakamura, K. Mitachi, Y. Kato, "Design study of small molten-salt fission power station suitable for coupling with accel. molten-salt breeders," *Emerging Nucl. Energy System*; 1986, *Proc. 4th ICENES*, Madrid, (Velarde, G., ed.), World Sci., Singapore, 235–239 (1987).
- 3) K. Furukawa *et al.*, "A road map for the realization of global-scale thorium breeding fuel cycle by single molten-fluoride flow, molten salt reactor for sustainable nuclear power-MSR FUJI," *ICENES 2007. 13th Int. Conf. on Emerging Nuclear Energy Systems*, June 3–8, 2007, Istanbul, Turkey (2007).
- 4) K. Mitachi, T. Suzuki, Y. Nakanishi, D. Okabayashi, "A preliminary design study of a small molten salt reactor for effective use of thorium resource," *Proc. 7th Int. Conf. on Nuclear Engineering*, Tokyo, Japan, 7144 (1999).
- 5) K. Mitachi, T. Suzuki, Y. Nakanishi, D. Okabayashi, R. Yoshioka, "Re-estimation of nuclear characteristics of a small molten salt power reactor," *Nihon-Genshiryoku-Gakkai Shi (J. At. Energy Soc. Jpn.)*, **42**[9], 99, (2000) [in Japanese].
- 6) R. Yoshioka, private communication.
- 7) Y. A. Chao, P. Huang, "Theory and performance of the fast-running multidimensional pressurized water reactor kinetics code," *SPNOVA-K. Nucl. Sci. Eng.*, **103**, 415 (1989).
- 8) K. Okumura, K. Kaneko, K. Tsuchihashi, "SRAC95: General purpose neutron code system," *JAERI-Data/Code*, 96-015 (1996) [in Japanese].
- 9) Y. Shimazu, "Nuclear safety analysis of a molten salt breeder reactor," *J. Nucl. Sci. Technol.*, **15**[7], 514–522 (1978).
- 10) <http://www.haynesintl.com>, Haynes International, Inc.
- 11) W. H. Jr. Sides, "Control study of a 1000-MW(e) MSBR," ORNL-TM-2927 (1970).
- 12) R. J. Kedel, A. Houtzeel, "Development of a model for computing ¹³⁵Xe migration in the MSRE," ORNL-4069 (1967).